PCCP

ROYAL SOCIETY OF CHEMISTRY

PAPER

View Article Online
View Journal | View Issue

Cite this: *Phys. Chem. Chem. Phys.*, 2021, **23**, 16629

Magnetically induced ring currents in naphthalene-fused heteroporphyrinoids†

Markus Rauhalahti,*[a] Dage Sundholm *[a] and Mikael P. Johansson *[ab]

Received 28th May 2021,
Accepted 10th July 2021

DOI: 10.1039/d1cp02381k

rsc.li/pccp

The magnetically induced current density of an intriguing naphthalene-fused heteroporphyrin has been studied, using the quantum-chemical, gauge-including magnetically induced currents (GIMIC) method. The ring-current strengths and current-density pathways for the heteroporphyrin, its Pd complex, and the analogous quinoline-fused heteroporphyrin provide detailed information about their aromatic properties. The three porphyrinoids have similar current-density pathways and are almost as aromatic as free-base porphyrin. Notably, we show that the global ring current makes a branch at three specific points. Thus, the global current is composed of a total of eight pathways that include 22 π-electrons, with no contributions from 18-electron pathways.

1 Introduction

The unique physico-chemical properties of porphyrinoids have led to comprehensive research activities proposing new porphyrinoids that can be employed in a variety of applications such as solar-energy conversion, homogeneous catalysis, the ability to form metal complexes, and in biomedicine.[1–9] Novel porphyrinoids are either synthesized *via* precursors to the target molecule or by modifying existing porphyrinoids. Recent experimental and computational studies of porphyrinoids have shown that significant changes in the aromatic properties and complexation properties can be obtained by synthesizing porphyrinoids whose π-electron conjugation and aromatic pathways significantly differ from those of naturally occurring porphyrins.[10–32]

Aromaticity is a steadily recurring theme when discussing the properties of porphyrinoids. The Hückel electron-count rule and the traditional 18π aromatic pathway[33–35] have played an important role in the design of novel porphyrinoids, even though the 18π conjugation pathway is often a too simplistic model of the aromatic properties of porphyrinoids.[36,37]

Molecular aromaticity is one of the fundamental concepts of chemistry, both descriptive and elusive at the same time; aromaticity is not a physical observable that can be unambiguously detected and quantified.[38–47] Among the most commonly used aromaticity indexes are those based on some magnetic criterion. Magnetic properties can be computed with high accuracy and are physical observables; nuclear magnetic resonance (NMR) spectra provide experimental information about the degree of aromaticity according to the magnetic or ring-current criterion.[38,40,48–62] In aromatic molecules, a homogeneous magnetic field perpendicular to the molecular ring induces a ring current in the classical direction, *i.e.*, in the diatropic direction. Antiaromatic molecules sustain a paratropic ring current flowing in the non-classical direction, and non-aromatic compounds sustain a vanishingly small net ring current. The induced ring current gives rise to a secondary magnetic field, which is a three-dimensional function that strengthens or weakens the applied magnetic field depending on whether the current density in the vicinity of the sample point flows in the paratropic or diatropic direction with respect to the sample point, respectively.[63] The presence of ring currents is often assessed indirectly through the induced magnetic field. Most common ways are measurements of ^{1}H NMR chemical shifts or calculations of nucleus-independent chemical shifts (NICS).[38] In NICS calculations, the shielding tensor at the centre of molecular rings is analysed. In more general NICS studies, the shielding tensor is calculated in many discrete points in the vicinity of the molecular ring.[54,55,64] For molecules consisting of connected molecular rings, the ambiguity arising from the complex current-density distribution makes the use of NICS based approaches less reliable.

Hong *et al.*[10] have synthesized porphyrinoids with a *meso*-fused naphthalene and one pyrrole moiety replaced by a thiophene ring. The molecule is interesting as it exhibits a cross-conjugated moiety, and presents a challenge for many of the topological descriptors and qualitative pictures of the aromatic conjugation pathway. Based on Nucleus-Independent Chemical Shift (NICS), structural

[a] *University of Helsinki, Department of Chemistry, Faculty of Science, P.O. Box 55 (A.I. Virtanens Plats 1), FI-00014 Helsinki, Finland.*
E-mail: Markus.Rauhalahti@helsinki.fi, Dage.Sundholm@helsinki.fi
[b] *CSC – IT Center for Science Ltd., P.O. Box 405, FI-02101 Espoo, Finland.*
E-mail: mikael.johansson@csc.fi

† Electronic supplementary information (ESI) available: Strengths of the current-density pathways calculated using the PBE0 and BHandHLYP funcionals and Cartesian coordinates of the optimized molecular structures and calculated NMR shieldings. See DOI: 10.1039/d1cp02381k

Harmonic Oscillator Stabilization Energy (HOSE) indices,[65] and Anisotropy of the Induced Current Density (AICD),[66] Hong *et al.* suggested that their molecules are either 18 or 22 π-electron conjugated systems; a definite answer could not be given, however. In addition, by calculating the isotropic component of the shielding tensor at the centre of the naphthalene rings, they found that the local aromaticity of the naphthalene is perturbed.

In this work, we set out to conclusively settle the question of the aromatic pathways for the Hong porphyrinoids. Do we have an 18 or 22 π-electron pathway? To this end, we have derived magnetically induced current densities using the GIMIC method[60,67–69] to elucidate the aromatic nature of the two synthesized novel porphyrinoids, and an analogous compound, in which the naphthalene moiety is replaced with a quinoline. The GIMIC method has been successfully used for assessing the degree of aromaticity in a number of molecules with complex molecular structures, including several porphyrinoids,[24,28,30–32,36,70–77] which have been recently reviewed.[78–80] The current pathways and ring-current strengths calculated using GIMIC yield unambiguous pictures of the aromatic character of complex molecules with many annelated molecular rings.

2 Methods

The starting geometries for the structural optimization of the free-base naphthalene-fused porphyrinoid (**1**) and the corresponding Pd complex (**2**) were taken from the crystal structure, and the quinoline-fused porphyrinoid (**3**) was created starting from the optimized structure of **2**. The molecular structures of **1–3** are shown in Fig. 1.

Aryl groups in the *meso*-positions were replaced by hydrogens to reduce the computational costs, since the aryl groups have little effect on the aromatic properties of the porphyrin core.[78] The structure optimizations and the calculations of the vibrational frequencies were performed at the density functional theory (DFT) level using the Becke–Perdew (BP) functional[81,82] and the resolution of identity (RI) approximation.[83,84] Dispersion interactions were considered using Grimme's method, employing Becke–Johnson damping (DFT-D3(BJ)).[85–87] In the optimization of the molecular structures, the def2-SVP basis sets and the corresponding effective core potential (ECP) for palladium were used.[88,89] Calculation of the harmonic vibrational frequencies showed that the obtained molecular structures are minima on the potential energy surfaces.[90] The coordinates of the optimized molecular structures are given in the ESI.†

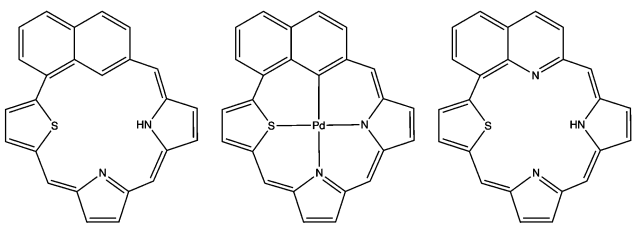

(a) (b) (c)

Fig. 1 Molecular structures of (a) **1**, (b) **2**, and (c) **3**.

The calculations show that the naphthalene-fused porphyrinoids **1** and **2** are non-planar with the thiophene ring tilted about 5–20 degrees out of the porphyrinoid plane, respectively, which is smaller than in previously studied heteroporphyrins.[31,73] The molecular structure of the quinoline analogue (**3**) is planar belonging to the C_s point group. Single-point energy calculations and nuclear magnetic resonance (NMR) shielding calculations were performed at the BP level using the def2-TZVP basis sets.[91] The NMR shielding calculation on **2** was also done with all-electron basis sets.[92] In order to corroborate the BP86 results, the magnetically induced current densities were also calculated with the non-empirical PBE0 functional[93,94] which has 25% Hartree–Fock exchange and with Becke's half-and-half functional (BHandHLYP, LIBXC ID 436) with the 50% Hartree–Fock exchange.[81,95,96] BHandHLYP was recently shown to yield the most accurate magnetisabilities of several functionals tested,[97] at least in the absence of explicit correction for self-interaction error (SIE).[98] Nuclear magnetic shieldings calculated using the BP functional are given in the ESI.†

Magnetically induced current densities were calculated with the GIMIC program.[60,67–69] GIMIC is an open-source tool for calculating and analysing current densities in open- and closed-shell molecules. Details about the use of the GIMIC method and its applications can be found on GitHub.[99] By numerically integrating the current density passing selected planes that cut chemical bonds, quantitative information about the strengths of the magnetically induced current susceptibilities and ring-current pathways is obtained. Integration planes were placed at the centre of the bonds of interest and oriented perpendicular to the bond. The integration plane begins in the vicinity of the current density vortex inside the studied bond and reaches far outside the molecule where the current density vanishes. The magnetic field was aligned along the integration plane, which is perpendicular to a plane through the *meso*-carbons. Small discrepancies in the current conservation are observed. The divergence of the current density does not completely vanish due to the use of a finite basis set. However, the main reason for the charge conservation problems originates most likely from the inner current-density vortex, which is not exactly perpendicular to the chosen molecular plane. The uncertainties in the strengths of the current-density pathways are small and do not affect the conclusions of this work.

The electronic structure and nuclear magnetic shielding calculations were performed with TURBOMOLE versions 7.0 and 7.5.[100,101] The calculations of the magnetically induced current density susceptibilities and ring current strength susceptibilities were performed with GIMIC 2.16. Figures were created with Chemcraft[102] and GIMP.[103] Below, magnetically induced current density susceptibilities are denoted current density for brevity.

3 Results and discussion

The current-density pathways and the ring-current strengths of **1**, **2**, and **3** computed with the BP functional are shown in Fig. 2. The porphyrinoids sustain a strong, global ring current of

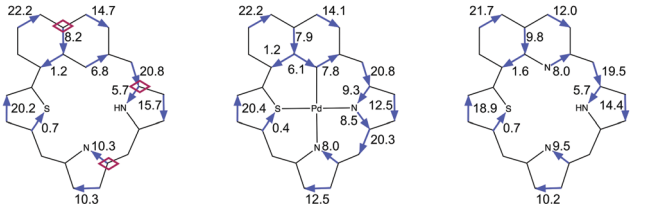

(a) (b) (c)

Fig. 2 Integrated current strengths (in nA T^{-1}) and current pathways of (a) **1**, (b) **2**, and (c) **3**. In (a), the three branch points of the current pathway are marked with purple diamond symbols.

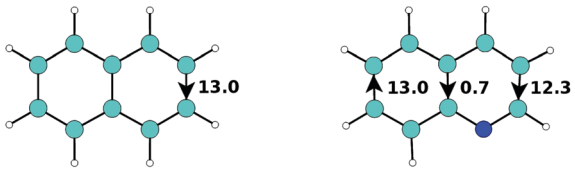

(a) (b)

Fig. 3 The integrated current-density strengths (in nA T^{-1}) and current-density pathways of (a) naphthalene and (b) quinoline.

20–21 nA T^{-1} around the porphyrinoid ring. The three molecules have very similar current-density pathways and current-density strengths. Compared to free-base porphyrins, with a ring-current of 27 nA T^{-1},[36] the ring-current strengths for **1**, **2**, and **3** are slightly smaller. A comparison to the arch-aromatic molecule benzene, with a ring-current strength of 12 nA T^{-1},[70] establishes all three species as strongly aromatic, however.

The currents crossing specific bonds paint a picture of the pathways that the currents traverse in the molecules. The first main observation is that in the porphyrinoids with annelated naphthalene and quinoline, the main current flows along the outer bonds of the two six-membered rings. This rules out the 18 π-electron pathway for these molecules, as the global current flow does not take the inner route at all. In fact, the six-membered ring closer to the thiophene ring sees a loss of local aromaticity, since only a weak diatropic ring current of 1.2–1.6 nA T^{-1} circles around that ring.

The global ring current splits at the other ring of the naphthalene or quinoline moiety. The current-density strength along the inner pathway is 6.8–8.0 nA T^{-1}, whereas 12.0–14.7 nA T^{-1} passes along the outer pathway. At the thiophene ring, the global ring current takes the outer route, with only a near-negligible current of 0.4–0.7 nA T^{-1} passes the sulphur atom.

At the pyrrolic rings, the ring current branches into outer and inner pathways. Hong *et al.* suggested that the outer $C_\beta{=}C_\beta$ bond of the pyrrolic rings without an inner hydrogen would be excluded from the aromatic pathway.[10] The present ring-current strength calculations show that the outer path is utilised, however. At the pyrrolic rings without inner hydrogens, the global ring current splits into two branches of almost equal magnitude. The current-density strength along the inner pathway is 8.0–10.3 nA T^{-1} while 10.2–12.5 nA T^{-1} takes the outer route. In the Pd complex, a weak local diatropic ring current of about 1 nA T^{-1} circles around the six-membered ring formed by Pd, the naphthalene moiety and the pyrrolic ring.

The ring-currents passing the pyrrolic nitrogens with an inner hydrogen show larger differences, 5.7 nA T^{-1} for the inner route, *vs.* 14.4–15.7 nA T^{-1} passing *via* the outer $C_\beta{=}C_\beta$ bond. Still, the current taking the inner route is non-negligible.

The currents are rather insensitive to the choice of density functional, in line with accrued experience on aromatic molecules;[104] the currents in anti-aromatic molecules tend to be more sensitive towards, *e.g.*, the amount of Hartree–Fock exchange. Here, PBE0 (25% HF exchange) and BHandHLYP (50% HF exchange) provide practically the same current strengths and pathways as the BP functional (no HF exchange). A minute difference in the ring current of the thiophene ring can be noted. The sulphur pathway is increasingly quenched with an increasing amount of HF exchange. With PBE0, the current passing the sulphur is practically zero; with BHandHLYP, the direction of the current is reversed compared to the BP results. In all cases, the current flow passing the sulphur atom is negligible (<1 nA T^{-1}). The current pathways calculated at the PBE0 and BHandHLYP levels are given in the ESI.†

For comparison, we also performed current density calculations on naphthalene and quinoline (Fig. 3). The GIMIC calculations show that the naphthalene molecule sustains a ring current of 13 nA T^{-1} around the whole molecule, whereas the strength of the net current passing the central C–C bond vanishes due to the symmetry.[69,105] Quinoline has a very similar current-density strength and pathway to naphthalene. Due to the broken symmetry, a weak current density of 0.7 nA T^{-1} passes the central C–C bond. The current-density strength passing the nitrogen-containing six-membered ring is 12.3 nA T^{-1}, whereas the current-density strength of the benzoic ring is 13 nA T^{-1}. Thus, the aromatic character of the annelated naphthalene and quinoline moieties of the studied porphyrinoids is quite different to those of the corresponding undecorated molecules, once again showing that the drastic effect that structural modification around aromatic centres can induce.

Finally, we highlight some observations regarding the ^{1}H NMR shieldings. The diatropic ring currents shift the ^{1}H NMR signal of the inner hydrogens in the upfield direction, that is, they are more shielded than the outer hydrogens, that in turn are downfield shifted. This effect is reflected in the obtained ^{1}H NMR shieldings. For molecule **1**, the signal of the inner hydrogen of the naphthalene moiety appears at 33.6 ppm and the isotropic shielding of the inner pyrrole hydrogen occurs at 32.9 ppm (calculated at the BHandHLYP level). The corresponding NMR signals of the *meso* hydrogens on the outside of the macrocycle are in the range of 21.2–22.4 ppm. For comparison, the tetramethylsilane (TMS) reference value is 31.8 ppm. The ring-current effect in molecule **1** is clearly seen in the *zz* component of the shielding tensor: 46.6 ppm and 45.8 ppm for the inner hydrogens of the naphthalene moiety and pyrrole, respectively, a significant upshift compared to the *zz* components of the outer *meso* hydrogens, which lie in the range of 8.5–10.9 ppm.

4 Conclusions

Ring-current strengths and ring-current pathways have been calculated for naphthalene- and quinoline-fused heteroporphyrins using

the GIMIC method. The studied porphyrinoids are aromatic according to the ring-current criterion, sustaining global ring currents of 20–21 nA T^{-1} around the porphyrinoid ring. The calculations show that the three heteroporphyrins have very similar current pathways and current-density strengths. The annelated naphthalene and quinoline moieties all but lose their local aromaticity. The six-membered ring of the naphthalene and quinoline moieties next to the thiophene sustains a very weak local ring current.

Along the global current pathway, the current makes a branch at three points (see Fig. 2). The ring current branches into an inner and outer pathway at the second six-membered ring of the naphthalene and quinoline moieties. About one third of the global ring-current takes the inner route. The ring current also splits into an inner and an outer branch at both pyrrolic rings. Almost no current passes the sulphur of the thiophene ring, however, so the current does not split further. For the pyrrolic ring without an inner hydrogen, the current-density strengths of the two branches are almost equally strong. About 25–40% of the global ring current passes the inner hydrogen of the pyrrolic ring.

The suggested 18 π-electron pathways can be ruled out, due to the weak local ring current of the benzoic ring next to the thiophene, which shows that the global ring current does not pass on the inside of that ring, necessarily lengthening the path.

Instead, we have a superposition of several 22 π-electron pathways (of which some are, formally, 21 and 23 electron pathways) that make up the total global induced π-electron current in the molecules. As the current branches into two streams at three distinct points of the macrocycle, we have in total eight 22 π-electron pathways. Of these, one was considered by Hong *et al.*,[10] while the second suggested 22-electron pathway can be ruled out on the same grounds as the 18-electron pathways.

We also note an alternative to the eight 22-electron pathways, namely a superposition of two 26-electron pathways (including one formally 25-electron pathway in the case of the Pd complex **2**, depending on how the π-electrons are counted). In this interpretation, the current would not bifurcate at the pyrrolic rings, but rather flow over the entire ring systems, due to their small size.

Summarising, of the sum total of 30 π-electrons in **1–3**, 28 are involved in the global ring current. The global current in turn is composed of a superposition of eight 22 π-electron pathways, or alternatively, two 26 π-electron pathways. In general, this study showcases the insight that can be obtained from directly following the current pathways of complex, multicycle molecules.

Author contributions

MR formulated the project scope, performed most of the calculations, and wrote the initial draft of the paper. All authors analysed the data, interpreted the results, and wrote the final manuscript.

Conflicts of interest

There are no conflicts to declare.

Acknowledgements

This work was supported by The Academy of Finland (projects 289179, 311149, 314821, and 319453), the Magnus Ehrnrooth Foundation, the Swedish Cultural Foundation in Finland, and Waldemar von Frenckells sitftelse. Ample computational resources granted by CSC – The Finnish IT Center for Science and the Finnish Grid and Cloud Infrastructure (urn:nbn:fi:research-infras-2016072533) are gratefully acknowledged.

References

1 C. Wang, H. Dong, W. Hu, Y. Liu and D. Zhu, *Chem. Rev.*, 2012, **112**, 2208–2267.
2 M. Jurow, A. E. Schuckman, J. D. Batteas and C. M. Drain, *Coord. Chem. Rev.*, 2010, **254**, 2297–2310.
3 T. Tanaka and A. Osuka, *Chem. Soc. Rev.*, 2015, **44**, 943–969.
4 J. Chou, M. E. Kosal, H. S. Nalwa, N. A. Rakow and K. S. Suslick, in *Porphyrin Handbook*, ed. K. M. Kadish, K. M. Smith, and R. Guilard, Academic Press, San Diego, CA, 2000, vol. **6**, pp. 41–128.
5 L.-L. Lia and E. Wei-Guang Diau, *Chem. Soc. Rev.*, 2013, **42**, 291–304.
6 R. Paolesse, S. Nardis, D. Monti, M. Stefanelli and C. Di Natale, *Chem. Rev.*, 2017, **117**, 2517–2583.
7 G. de la Torre, G. Bottari, M. Sekita, A. Hausmann, D. M. Guldi and T. Torres, *Chem. Soc. Rev.*, 2013, **42**, 8049–8105.
8 H. Lu and N. Kobayashi, *Chem. Rev.*, 2016, **116**, 6184–6261.
9 J. Mack, *Chem. Rev.*, 2017, **117**, 3444–3478.
10 J.-H. Hong, A. S. Aslam, M. Ishida, S. Mori, H. Furuta and D.-G. Cho, *J. Am. Chem. Soc.*, 2016, **138**, 4992–4995.
11 J. L. Sessler and D. Seidel, *Angew. Chem., Int. Ed.*, 2003, **42**, 5134–5175.
12 M. O. Senge, *Angew. Chem., Int. Ed.*, 2011, **50**, 4272–4277.
13 K. Berlin, *Angew. Chem., Int. Ed. Engl.*, 1996, **35**, 1820–1822.
14 T. D. Lash and S. T. Chaney, *Chem. – Eur. J.*, 1996, **2**, 944–948.
15 A. Berlicka, P. Dutka, L. Szterenberg and L. Latos-Grażyński, *Angew. Chem., Int. Ed.*, 2014, **53**, 4885–4889.
16 B. Szyszko, L. Latos-Grażyński and L. Szterenberg, *Angew. Chem., Int. Ed.*, 2011, **50**, 6587–6591.
17 T. D. Lash, M. J. Hayes, J. D. Spence, M. A. Muckey, G. M. Ferrence and L. F. Szczepura, *J. Org. Chem.*, 2002, **67**, 4860–4874.
18 T. D. Lash, *Eur. J. Org. Chem.*, 2007, 5461–5481.
19 D. I. AbuSalim and T. D. Lash, *J. Org. Chem.*, 2013, **78**, 11535–11548.
20 M. Pawlicki and L. Latos-Grażyński, *Chem. Rec.*, 2006, **6**, 64–78.
21 A. Ghosh, *Angew. Chem., Int. Ed.*, 2004, **43**, 1918–1931.
22 D. Li and T. D. Lash, *J. Org. Chem.*, 2014, **79**, 7112–7121.

23 T. D. Lash, G. C. Gilot and D. I. AbuSalim, *J. Org. Chem.*, 2014, **79**, 9704–9716.
24 H. Fliegl, D. Sundholm, S. Taubert and F. Pichierri, *J. Phys. Chem. A*, 2010, **114**, 7153–7161.
25 H. Fliegl, D. Sundholm and F. Pichierri, *Phys. Chem. Chem. Phys.*, 2011, **13**, 20659–20665.
26 H. Fliegl, N. Özcan, R. Mera-Adasme, F. Pichierri, J. Jusélius and D. Sundholm, *Mol. Phys.*, 2013, **111**, 1364–1372.
27 R. R. Valiev, H. Fliegl and D. Sundholm, *J. Phys. Chem. A*, 2013, **117**, 9062–9068.
28 R. R. Valiev and V. N. Cherepanov, *Int. J. Quantum Chem.*, 2013, **113**, 2563–2567.
29 H. Fliegl, F. Pichierri and D. Sundholm, *J. Phys. Chem. A*, 2015, **0**, 2344–2350.
30 R. R. Valiev, H. Fliegl and D. Sundholm, *Phys. Chem. Chem. Phys.*, 2014, **16**, 11010–11016.
31 R. R. Valiev, H. Fliegl and D. Sundholm, *J. Phys. Chem. A*, 2015, **119**, 1201–1207.
32 R. R. Valiev, H. Fliegl and D. Sundholm, *Phys. Chem. Chem. Phys.*, 2015, **17**, 14215–14222.
33 F. Sondheimer, R. Wolovsky and Y. Amiel, *J. Am. Chem. Soc.*, 1962, **84**, 274–284.
34 E. Vogel, *Pure Appl. Chem.*, 1993, **65**, 143–152.
35 T. D. Lash, *J. Porphyrins Phthalocyanines*, 2011, **15**, 1093–1115.
36 H. Fliegl and D. Sundholm, *J. Org. Chem.*, 2012, **77**, 3408–3414.
37 A. S. Ivanov and A. I. Boldyrev, *Org. Biomol. Chem.*, 2014, **12**, 6145–6150.
38 P. von Ragué Schleyer, C. Maerker, A. Dransfeld, H. Jiao and N. J. R. van Eikema Hommes, *J. Am. Chem. Soc.*, 1996, **118**, 6317–6318.
39 P. von Ragué Schleyer and H. Jiao, *Pure Appl. Chem.*, 1996, **28**, 209–218.
40 A. Balaban, P. von Ragué Schleyer and H. S. Rzepa, *Chem. Rev.*, 2005, **105**, 3436–3447.
41 P. von Ragué Schleyer, M. Manoharan, Z.-X. Wang, B. Kiran, H. Jiao, R. Puchta and N. J. R. van Eikema Hommes, *Org. Lett.*, 2001, **3**, 2465–2468.
42 T. M. Krygowski and M. K. Cyrański, *Chem. Rev.*, 2001, **101**, 1385–1420.
43 P. Lazzeretti, *Phys. Chem. Chem. Phys.*, 2004, **6**, 217–223.
44 M. K. Cyrański, P. von Ragué Schleyer, T. M. Krygowski, H. Jiao and G. Hohlneicher, *Tetrahedron*, 2003, **59**, 1657–1665.
45 R. Hoffmann, *Am. Sci.*, 2015, **103**, 18–22.
46 M. Solá, *Front. Chem.*, 2017, **5**, 22.
47 C. Kumar, H. Fliegl and D. Sundholm, *J. Phys. Chem. A*, 2017, **121**, 7282–7289.
48 J. A. Pople, *Mol. Phys.*, 1958, **1**, 175–180.
49 R. McWeeny, *Mol. Phys.*, 1958, **1**, 311–321.
50 J. A. Elvidge and L. M. Jackman, *J. Chem. Soc.*, 1961, 859.
51 J. A. Elvidge, *Chem. Commun.*, 1965, 160–161.
52 R. Du Vernet and V. Boekelheide, *Proc. Natl. Acad. Sci. U. S. A.*, 1974, **71**, 2961–2964.
53 S. Klod and E. Kleinpeter, *J. Chem. Soc., Perkin Trans. 2*, 2001, 1893–1898.
54 S. Klod, A. Koch and E. Kleinpeter, *J. Chem. Soc., Perkin Trans. 2*, 2002, 1506–1509.
55 G. Merino, T. Heine and G. Seifert, *Chem. – Eur. J.*, 2004, **10**, 4367–4371.
56 G. Merino, A. Vela and T. Heine, *Chem. Rev.*, 2005, **105**, 3812–3841.
57 C. S. Wannere, C. Corminboeuf, W. D. Allen, H. F. Schaefer III and P. von Ragué Schleyer, *Org. Lett.*, 2005, **7**, 1457–1460.
58 R. Herges and D. Geuenich, *J. Phys. Chem. B*, 2001, **105**, 3214–3220.
59 D. Geuenich, K. Hess, F. Kohler and R. Herges, *Chem. Rev.*, 2005, **105**, 3758–3772.
60 J. Jusélius, D. Sundholm and J. Gauss, *J. Chem. Phys.*, 2004, **121**, 3952–3963.
61 Z. Chen, C. S. Wannere, C. Corminboeuf, R. Puchta and P. von Ragué Schleyer, *Chem. Rev.*, 2005, **105**, 3842–3888.
62 J. A. N. F. Gomes and R. B. Mallion, *Chem. Rev.*, 2001, **101**, 1349–1384.
63 R. K. Jinger, H. Fliegl, R. Bast, M. Dimitrova, S. Lehtola and D. Sundholm, *J. Phys. Chem. A*, 2021, **125**, 1778–1786.
64 J. Jusélius and D. Sundholm, *Phys. Chem. Chem. Phys.*, 1999, **1**, 3429–3435.
65 T. M. Krygowski and T. Wieckowski, *Croat. Chem. Acta*, 1981, **54**, 193–202.
66 D. Geuenich, K. Hess, F. Köhler and R. Herges, *Chem. Rev.*, 2005, **105**, 3758–3772.
67 S. Taubert, D. Sundholm and J. Jusélius, *J. Chem. Phys.*, 2011, **134**, 054123.
68 H. Fliegl, S. Taubert, O. Lehtonen and D. Sundholm, *Phys. Chem. Chem. Phys.*, 2011, **13**, 20500–20518.
69 D. Sundholm, H. Fliegl and R. J. Berger, *Wiley Interdiscip. Rev.: Comput. Mol. Sci.*, 2016, **6**, 639–678.
70 M. P. Johansson and J. Jusélius, *Lett. Org. Chem.*, 2005, **2**, 469–474.
71 M. P. Johansson, J. Jusélius and D. Sundholm, *Angew. Chem., Int. Ed.*, 2005, **44**, 1843–1846.
72 M. P. Johansson, *J. Phys. Chem. C*, 2009, **113**, 524–530.
73 J. Ren, F.-Q. Bai and H.-X. Zhang, *Int. J. Quantum Chem.*, 2015, **115**, 983–988.
74 I. Benkyi, H. Fliegl, R. R. Valiev and D. Sundholm, *Phys. Chem. Chem. Phys.*, 2016, **18**, 11932–11941.
75 R. Nozawa1, J. Kim, J. Oh, A. Lamping, Y. Wang, S. Shimizu, I. Hisaki, T. Kowalczyk, H. Fliegl, D. Kim and H. Shinokubo, *Nat. Commun.*, 2019, **10**, 3576.
76 S. G. Patra and N. Mandal, *Int. J. Quantum Chem.*, 2020, **120**, e26152.
77 O. López-Estrada, B. Zuniga-Gutierrez, E. Selenius, S. Malola and H. Häkkinen, *Nat. Commun.*, 2021, **12**, 2477.
78 H. Fliegl, R. R. Valiev, F. Pichierri and D. Sundholm, *Chem. Modell.*, 2018, **14**, 1–42.
79 D. Sundholm and H. Fliegl, in *Handbook of Porphyrin Science*, ed. K. M. Kadish, K. M. Smith and R. Guilard, World Scientific, 2021, vol. **46**, in press.

80 M. Dimitrova and D. Sundholm, in *Aromaticity: Modern Computational Methods and Applications*, ed. I. F. López, Elsevier, Amsterdam, Netherlands, 2021, ch. 5, pp. 41–128.
81 A. D. Becke, *Phys. Rev. A: At., Mol., Opt. Phys.*, 1988, **38**, 3098–3100.
82 J. P. Perdew, *Phys. Rev. B: Condens. Matter Mater. Phys.*, 1986, **33**, 8822–8824.
83 K. Eichkorn, O. Treutler, H. Öhm, M. Häser and R. Ahlrichs, *Chem. Phys. Lett.*, 1995, **240**, 283–289.
84 K. Eichkorn, F. Weigend, O. Treutler and R. Ahlrichs, *Theor. Chem. Acc.*, 1997, **97**, 119–124.
85 S. Grimme, J. Antony, S. Ehrlich and H. Krieg, *J. Chem. Phys.*, 2010, **132**, 154104.
86 S. Grimme, S. Ehrlich and L. Goerigk, *J. Comput. Chem.*, 2011, **32**, 1456–1465.
87 A. D. Becke and E. R. Johnson, *J. Chem. Phys.*, 2005, **123**, 154101.
88 A. Schäfer, H. Horn and R. Ahlrichs, *J. Chem. Phys.*, 1992, **97**, 2571–2577.
89 D. Andrae, U. Häußermann, M. Dolg, H. Stoll and H. Preuß, *Theor. Chim. Acta*, 1990, **77**, 123–141.
90 P. Deglmann and F. Furche, *Chem. Phys. Lett.*, 2002, **362**, 511–518.
91 F. Weigend and R. Ahlrichs, *Phys. Chem. Chem. Phys.*, 2005, **7**, 3297–3305.
92 R. Ahlrichs and K. May, *Phys. Chem. Chem. Phys.*, 2000, **2**, 943–945.
93 J. P. Perdew, K. Burke and M. Ernzerhof, *J. Chem. Phys.*, 1996, **105**, 9982–9985.
94 C. Adamo and V. Barone, *J. Chem. Phys.*, 1999, **110**, 6158–6170.
95 A. D. Becke, *J. Chem. Phys.*, 1993, **98**, 1372–1377.
96 C. Lee, W. Yang and R. G. Parr, *Phys. Rev. B: Condens. Matter Mater. Phys.*, 1988, **37**, 785–789.
97 S. Lehtola, M. Dimitrova, H. Fliegl and D. Sundholm, *J. Chem. Theory Comput.*, 2021, **17**, 1457–1468.
98 M. P. Johansson and M. Swart, *J. Chem. Theory Comput.*, 2010, **6**, 3302–3311.
99 GIMIC, version 2.0, a current density program, Can be freely downloaded from https://github.com/qmcurrents/gimic.
100 R. Ahlrichs, M. Bär, M. Häser, H. Horn and C. Kölmel, *Chem. Phys. Lett.*, 1989, **162**, 165–169.
101 F. Furche, R. Ahlrichs, C. Hättig, W. Klopper, M. Sierka and F. Weigend, *Wiley Interdiscip. Rev.: Comput. Mol. Sci.*, 2014, **4**, 91–100.
102 G. A. Zhurko and D. A. Zhurko, Chemcraft – graphical software for visualization of quantum chemistry computations, http://www.chemcraftprog.com/.
103 The GIMP Development Team, https://www.gimp.org, version: 2.10.12, date: 2019-06-12.
104 R. R. Valiev, I. Benkyi, Y. V. Konyshev, H. Fliegl and D. Sundholm, *J. Phys. Chem. A*, 2018, **122**, 4756–4767.
105 M. Dimitrova and D. Sundholm, *Phys. Chem. Chem. Phys.*, 2018, **20**, 1337–1346.

